The Journal of Experimental Biology 203, 2851–2863 (2000)
Printed in Great Britain © The Company of Biologists Limited 2000
JEB2975

THE MECHANICS OF LOCOMOTION IN THE SQUID *LOLIGO PEALEI*: LOCOMOTORY FUNCTION AND UNSTEADY HYDRODYNAMICS OF THE JET AND INTRAMANTLE PRESSURE

ERIK J. ANDERSON* AND M. EDWIN DEMONT‡

Biology Department, St Francis Xavier University, PO Box 5000, Antigonish, Nova Scotia, Canada B2G 2W5

*Present address: Department of Applied Ocean Physics and Engineering, Woods Hole Oceanographic Institution, Woods Hole, MA 02543, USA

‡Author for correspondence (e-mail: edemont@stfx.ca)

Accepted 14 June; published on WWW 22 August 2000

Summary

High-speed, high-resolution digital video recordings of swimming squid (*Loligo pealei*) were acquired. These recordings were used to determine very accurate swimming kinematics, body deformations and mantle cavity volume. The time-varying squid profile was digitized automatically from the acquired swimming sequences. Mantle cavity volume flow rates were determined under the assumption of axisymmetry and the condition of incompressibility. The data were then used to calculate jet velocity, jet thrust and intramantle pressure, including unsteady effects. Because of the accurate measurements of volume flow rate, the standard use of estimated discharge coefficients was avoided. Equations for jet and whole-cycle propulsive efficiency were developed, including a general equation incorporating unsteady effects.

Squid were observed to eject up to 94 % of their intramantle working fluid at relatively high swimming speeds. As a result, the standard use of the so-called large-reservoir approximation in the determination of intramantle pressure by the Bernoulli equation leads to significant errors in calculating intramantle pressure from jet velocity and *vice versa*. The failure of this approximation in squid locomotion also implies that pressure variation throughout the mantle cannot be ignored. In addition, the unsteady terms of the Bernoulli equation and the momentum equation proved to be significant to the determination of intramantle pressure and jet thrust. Equations of propulsive efficiency derived for squid did not resemble Froude efficiency. Instead, they resembled the equation of rocket motor propulsive efficiency. The Froude equation was found to underestimate the propulsive efficiency of the jet period of the squid locomotory cycle and to overestimate whole-cycle propulsive efficiency when compared with efficiencies calculated from equations derived with the squid locomotory apparatus in mind. The equations for squid propulsive efficiency reveal that the refill period of squid plays a greater role, and the jet period a lesser role, in the low whole-cycle efficiencies predicted in squid and similar jet-propelled organisms. These findings offer new perspectives on locomotory hydrodynamics, intramantle pressure measurements and functional morphology with regard to squid and other jet-propelled organisms.

Key words: locomotion, swimming, squid, *Loligo pealei*, jet propulsion, hydrodynamics, efficiency, mantle, cephalopod.

Introduction

Squid swim using a jet propulsion system and undulating fins. Fig. 1 illustrates the basic structures and mechanism of jet propulsion in these marine invertebrates. Water in the mantle cavity of the squid is pressurized by the powerful contraction of muscles running circumferentially in the mantle wall. That water is then expelled as a jet near the head of the animal. The muscles that power this jet are called the circular muscles. The squid is propelled mantle-first, arms trailing through the water. This is actually rearward swimming with respect to squid anatomy and is the norm in sustained swimming. Nevertheless, squid are able to propel themselves in various directions by muscularly directing their jet. Squid sometimes swim arms-leading for extended periods. Arms-leading swimming is common during feeding. After jetting, the squid refills its mantle cavity with sea water to prepare for the next jet period. Refilling of the mantle is believed to be driven by a combination of the elastic properties of the mantle tissue (Gosline and Shadwick, 1983), the action of antagonistic muscles called radial muscles (Gosline et al., 1983) and flow-induced surface pressures (Vogel, 1987). The intake and jetting of water are regulated by a structure known as the funnel, which acts as a one-way valve.

Squid also display a behavior known as escape jetting, which is used to escape predators and other dangers. In this behavior, the squid hyperinflates the mantle, increasing its resting mantle cavity volume, and then contracts the mantle

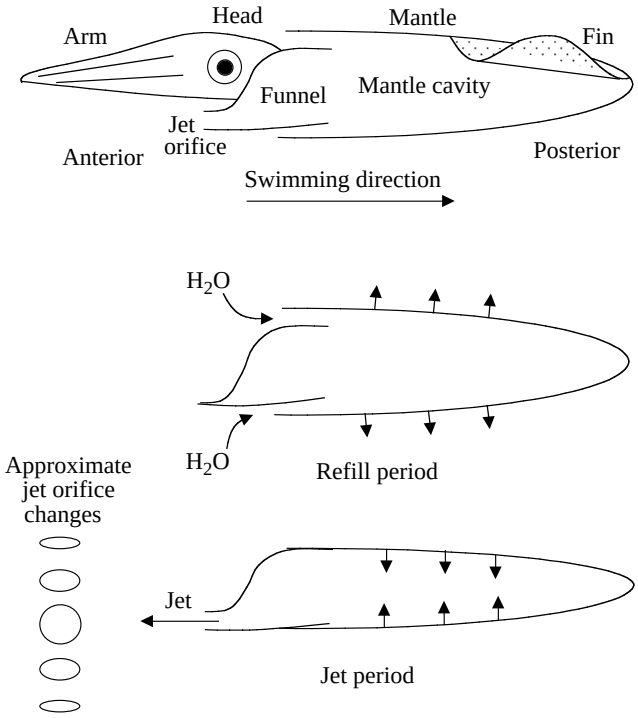

Fig. 1. Structure and mechanics of squid propulsion. Small arrows indicate the motion of the mantle wall during the jet and refill periods. During the jet period, the jet orifice is approximated by an ellipse of constant major axis and variable minor axis, based on video data (S. Foster and R. K. O'Dor, personal communication). The jet orifice is closed during refilling.

powerfully (Gosline and DeMont, 1985). This process is usually repeated a few times when the squid is attempting to escape danger. Since squid expel a large proportion of their working fluid in escape jetting, an analysis of escape jetting would be subject to the same problems arising from a steady hydrodynamic analysis of jet propulsion and the large-reservoir approximation (see Summary). In this investigation, however, the focus is on jet periods during sustained swimming, as would be observed during migrations. *Todarodes pacificus*, a squid of comparable size to *Loligo pealei*, has been observed to migrate at speeds of approximately 0.30 m s^{-1} for 2–3 months (Shevtsov, 1973).

This study is part of a comprehensive investigation of squid locomotion. This portion of the work focuses on the locomotory function and unsteady hydrodynamics of the jet and intramantle pressure. The complete work characterizes (i) the kinematics and strain history of the mantle, (ii) the locomotory function of the fins, (iii) a whole-body kinematic and dynamic analysis (Anderson, 1998), and (iv) the physical properties of the mantle (MacGillivray et al., 1999).

Materials and methods

Animals

Specimens of *Loligo pealei* (LeSueur) were captured in Woods Hole Sound, Massachusetts, USA, and cared for at the Marine Resources Center (MRC), located at Woods Hole Marine Biological Laboratory (MBL), as described elsewhere (Anderson, 1998). Squid were swum in flumes at the Woods Hole Oceanographic Institution Rhinehart Coastal Research Center. Water temperature in the flumes ranged from 12 to 15 °C. These temperatures are within the range experienced by *L. pealei* in the wild. High-speed video recordings of squid swimming mantle-leading were taken using a Redlake HR500 Motionscope. Lateral and dorsal views of steady swimming were recorded at the same flume speeds but not, however, simultaneously. One bout of arms-leading swimming was recorded. The camera was operated at 125 or 250 frames s^{-1} and stored up to 512 frames per sequence, allowing for video sequences of 4 and 2 s in duration, respectively. The video image resolution was 600 pixels×480 pixels. After an acceptable video sequence had been recorded, it was downloaded from the camera's RAM to a PC using a National Instruments, IMAQ PCI-1408 frame-grabber, LabVIEW and IMAQ Vision (Graftek).

Data collected from two squid, considered to be representative of more than 30 sequences taken from 10 squid, are reported in this paper. For ease, these two squid will be referred to as squid 1 and squid 2. Morphometrics for the two squid are: (1) squid 1: length 0.356 m, mantle length 0.25 m, wet mass 0.169 kg; (2) squid 2: length 0.313 m, mantle length 0.222 m, wet mass 0.183 kg. The notation squid 1s will be used to represent squid 1 swimming slowly (0.25 m s^{-1}), and squid 1f will be used to represent squid 1 swimming fast (0.43 m s^{-1}). Squid 2f represents squid 2 swimming fast (0.38 m s^{-1}).

Mantle volume

Squid swimming sequences were analyzed automatically with a PC, frame-by-frame, using a peak gray-level gradient-searching algorithm (Anderson, 1998). The algorithm subjects images to a standard Prewitt gradient filter and then searches the gradient matrix for the contour of maximum gradient that represents the outline of the squid. This works well for high-contrast image sequences. Good contrast was achieved using front lighting and a black felt background. Sequences of digital, *in vivo* squid outlines were then used to make accurate calculations of volumetric flow into and out of the squid. The incompressibility of squid tissue and sea water requires that any measured change in whole-mantle volume is accompanied by an equivalent change in mantle cavity water volume. Mantle volume, $\forall_m(t)$, was calculated from the squid outline data using:

$$\forall_m(t) = \frac{\pi}{4}\int_0^{L_m} [D(\xi,t)]^2\, d\xi , \qquad (1)$$

where L_m is the mantle length and $D(\xi,t)$ is the squid diameter at position ξ along the squid at any time, t. The axial position, ξ, is measured from the leading end of the squid. The integral was solved using either the trapezoid rule or an analytical integration of a fitted polynomial curve. Volumes calculated using the two techniques differed by less than 0.5 ml, i.e. less

than 1 % of resting mantle cavity volume. Note that the squid is treated as axisymmetric. Deviations from axisymmetry could lead to over- or underpredictions of volume flow. These errors depend on differences in strain histories in various longitudinal planes through the mantle.

$$Q(t) = -\frac{\mathrm{d}\forall_{\mathrm{m}}(t)}{\mathrm{d}t}\,. \tag{2}$$

As is conventional in fluid dynamics, negative values represent flow into the mantle. Volume flow rate determined by this method bypasses the use of so-called discharge coefficients, C_{d}, which range from 0 to 1 and are used when estimating volume flow rate on the basis of intramantle pressure recordings. This represents an important advance in quantitative analysis of squid jet propulsion. Volume flow rate affects nearly all the variables of interest in jet propulsion, and discharge coefficients are highly speculative. In the past, investigators have suggested a wide range of values of C_{d} for squid, from 0.6 to 1.0 (Johnson and Soden, 1966; Johnson et al., 1972; O'Dor, 1988a,b), representing a large uncertainty in volume flow rate.

Approximate resting mantle cavity volume, $\forall_{\mathrm{R}}$, was assumed to be the volume of water needed to fill the mantle of a dead squid with gills and viscera still intact. There is possibly a slight overestimation caused by hydrostatic pressure expanding the mantle during the measurement. Mantle cavity volume, $\forall_{\mathrm{C}}(t)$, was then calculated by:

$$\forall_{\mathrm{C}}(t) = \forall_{\mathrm{R}} + \forall_{\mathrm{m}}(t) - \forall_{\mathrm{max}}, \tag{3}$$

where $\forall_{\mathrm{max}}$ is the maximum volume of the $\forall_{\mathrm{m}}(t)$ curve. That is, when the mantle volume was at its maximum value, the mantle cavity volume was assumed to be at resting volume. No hyperinflation was observed in our swimming sequences. In an analysis of escape jetting, hyperinflation would require a more careful definition of resting volume (Gosline and DeMont, 1985).

Jet velocity

Volume flow rate and jet orifice area can be used to calculate jet velocity, which is necessary to determine subsequent variables such as intramantle pressure, jet thrust and propulsive efficiency. Jet orifice area was determined as follows. In lateral views of squid, the profile of the jet orifice is visible. The time-dependent length of the orifice profile was measured. Image sequences of the jet orifice of jetting squid show that the opening goes from a horizontal slit to a nearly circular shape (S. Foster and R. K. O'Dor, personal communication). The horizontal dimension appears to change very little through the opening process, and the intermediate shapes are therefore approximately elliptical (Fig. 1). In the light of this observation, jet area, $A_{\mathrm{j}}(t)$, was calculated using the time-varying jet profile length as the minor axis, $b(t)$, of an ellipse. The maximum profile length was used as the constant, horizontal major axis, a.

$$A_{\mathrm{j}}(t) = \frac{\pi}{4}\,ab(t)\,. \tag{4}$$

Jet flow velocity, $V_{\mathrm{j}}(t)$, was calculated using the following equation:

$$V_{\mathrm{j}}(t) = \frac{Q(t)}{A_{\mathrm{j}}(t)}\,. \tag{5}$$

Note that this equation assumes an ideal, uniform velocity profile over the jet orifice. In reality, equation 5 yields the average jet velocity over the orifice at a given time since the velocity profile can be expected to deviate somewhat from the ideal. The calculated jet velocity is not, however, simply the average jet velocity over the entire jet period, and so will not be referred to as average velocity. The direction of jet flow was assumed to be perpendicular to the straight-line jet orifice profile, i.e. roughly opposite to the swimming direction. The time-varying angle of the orifice to the long axis of the squid was measured over complete jet periods and used in determining the role of the jet in the balance of forces (Anderson, 1998). Note that the term 'jet velocity', which suggests a vector quantity, tends, in the literature, to be used for jet flow speed (a scalar) and strict jet velocity, interchangeably. Equation 5 technically yields jet flow speed. Jet velocity, in this paper, is defined as positive in the direction in which the jet is pointed. Equations 2 and 5 are conveniently in accord with this sign convention.

Propulsive efficiency

Jet propulsive efficiencies depend on jet velocity in comparison with the velocity of the flow past the propelled vehicle. If the jet flow velocity is much greater than the flow past the body, a large amount of kinetic energy is wasted in swirling fluid behind the body. It is important to note that propulsive efficiency is simply hydrodynamic efficiency for which forward thrust is considered useful work. Internal losses due to metabolism and internal friction are not included. These are needed to calculate total locomotory efficiency. Propulsive efficiency, therefore, represents an upper bound for total efficiency.

Several investigators in the past have applied the equation of Froude efficiency, which originates from a control volume analysis of an airscrew-like propeller, to calculate propulsive efficiency in jet-propelled organisms such as squid and scallops (Cheng and DeMont, 1996; Vogel, 1994; Webber and O'Dor, 1986). The equation for the Froude efficiency η_{f} is:

$$\eta_{\mathrm{f}} = \frac{2V}{V + V_{\mathrm{j}}} = \frac{V}{V + (\Delta V/2)}\,;\; \Delta V = V_{\mathrm{j}} - V\,, \tag{6}$$

where V is the velocity of the fluid far upstream of the propeller with respect to the propeller and V_{j} is the velocity of the jet downstream from the propeller with respect to the propeller (Prandtl, 1952). Both V and V_{j} point in the downstream direction, parallel to the axis of rotation of the airscrew, and are positive quantities in that direction. V may also be thought of as the velocity of the airscrew through a still fluid. In this case, V is positive in the direction of motion through the fluid. The increase in velocity of the fluid as it moves from upstream to downstream is ΔV. This change in fluid momentum is the origin of thrust. Ideal, steady flow is assumed.

If the same methods and assumptions are applied to derive

the propulsive efficiency of a squid, paying attention only to the time when the jet is being produced, a different equation arises:

$$\eta_j = \frac{2VV_j}{V^2 + V_j^2}, \quad (7)$$

where V is the velocity of the flow past the body, η_j is the propulsive efficiency during the jet period and V_j is the jet velocity relative to the body. This equation is none other that the equation of rocket motor propulsive efficiency (Streeter and Wylie, 1985; Houghton and Carpenter, 1993). This is not surprising since, during jetting, the squid is essentially a rocket. Propulsive efficiency was calculated using both equations (equations 6 and 7) and compared. The angle at which the jet was emitted was also factored into the efficiency by using only the axial component of the jet velocity in the efficiency calculation since the flow past the squid was essentially in the axial direction. The transverse component of the jet would tend to decrease the efficiencies calculated using equations 6 and 7, but preliminary approximations using the data from this investigation suggest that the effect would decrease the efficiencies by less than 4%. Any differences between efficiency calculated from the Froude and rocket equations would, nevertheless, remain.

It is arguable that Froude efficiency and rocket efficiency applied to squid should not be compared. Froude efficiency encompasses working fluid intake and output, while rocket propulsive efficiency only deals with working fluid output. Fluid intake, or refill, in squid obviously decreases locomotory efficiency, and Froude efficiency generally results in lower calculated efficiencies than the rocket equation. Therefore, it is tempting to suggest that Froude efficiency is the more appropriate method for calculating whole-cycle propulsive efficiency in squid. However, a close look at Froude efficiency reveals that it claims that no losses occur due to intake. In contrast, consideration of the complete locomotory cycle of a swimming squid results in:

$$\eta = \frac{2VV_j}{2V_R V + 3V^2 + V_j^2}, \quad (8)$$

where V_R is the velocity of fluid flowing into the squid during refilling at the intake orifice and η is whole-cycle propulsive efficiency. The equation reveals two very important pieces of information. First, whole-cycle propulsive efficiency in squid has a theoretical limit of 58%. This is approached when V_R is small and V_j=1.7V. Second, the efficiency equation is more similar to the rocket efficiency equation than to the Froude efficiency equation. The denominator of equation 8 differs from rocket efficiency by $2V_R V$+$2V^2$. These terms arise entirely from the refill period of the squid locomotory cycle. The velocity of the fluid taken into the mantle is changed by V+V_R at the refill orifice. Some of the momentum is inevitably recaptured since the fluid, once inside the mantle, is decelerated by V_R. The recaptured momentum would have a relatively small impact on efficiency and would not change the upper limit of 58%. Instead, it could raise slightly the lower limits of efficiency at higher refill rates observed at higher swimming speeds (Webber and O'Dor, 1986). But losses during the deceleration of the fluid in the mantle could cancel or outweigh the small efficiency-enhancing thrust that is produced.

In short, Froude efficiency tends to underpredict efficiency during jetting and, compared with whole-cycle efficiency, it fails to incorporate the real effects of the intake mechanism of squid. It will be shown in the Results section that this failure causes Froude efficiency to overpredict whole-cycle propulsive efficiency. Froude efficiency also predicts periodic occurrences of efficiencies greater than 100% in swimming squid. Neither the rocket efficiency equation nor the squid whole-cycle efficiency equation results in efficiencies greater than 100%.

The same case can be made against Froude efficiency for the jet-propelled scallop. Under the assumption of a simple refill mechanism in which fluid more-or-less passively fills the space between the opening valves as the organism moves forwards, whole-cycle propulsive efficiency is:

$$\eta = \frac{2VV_j}{3V^2 + V_j^2}, \quad (9)$$

As for squid, the upper limit of efficiency is 58%, but since it was assumed that no additional momentum had to be imparted to the fluid to pull it into the space between the valves, the term $2V_R V$, from equation 8, is not present, and efficiency is greater. In fact, if the recoil of the abducting 'spring' in the scallop hinge is powerful enough during swimming to produce a suction during refilling, a small thrust force would result that could increase efficiency, however slightly. Losses during the deceleration of this fluid in the fluid chamber may negate this effect. If, instead, the valves require a significant amount of fluid impact to open, efficiency would be decreased. A combination of these effects probably occurs in scallops. For example, refill by suction is certainly required during lift-off.

The equations of propulsive efficiency presented above all assume ideal, steady flow. The actual propulsive efficiency of squid swimming at a constant average velocity requires an equation that incorporates real fluid and unsteady effects. This equation takes the form:

$$\eta = \frac{W}{E_R + E_w + W}, \quad (10)$$

where W is the work done to overcome drag during one locomotory cycle, E_w is total fluid kinetic energy in the wake due to the jet and E_R is energy wasted in the process of refilling. Several measurements are necessary before this equation can be used to calculate efficiency in squid: time-varying drag, swimming velocity, wake flow visualization, refill velocity and refill orifice area.

Jet thrust and intramantle pressure

Jet thrust F was calculated using the so-called momentum equation (Batchelor, 1987), including the unsteady term:

$$F = \frac{\partial}{\partial t}\int_{C\forall} V(x,t)\rho \mathrm{d}\forall + \int_{CS} V(x,t)\rho V(x,t)\mathrm{d}A\,, \qquad (11)$$

where $V(x,t)$ is the fluid velocity inside the swimming squid (the control volume, $C\forall$), ρ is the fluid density, $\mathrm{d}\forall$ is an incremental volume in the intramantle fluid and $\mathrm{d}A$ is an incremental area over the walls of the mantle cavity (the control surface, *CS*). The squid mantle cavity was assumed to be a cylinder of constant length chosen on the basis of the region of the mantle exhibiting the bulk of diameter changes (Anderson, 1998). The diameter of the cylinder was prescribed by the measured volume flow. Fluid velocities in the mantle were calculated as a function of axial position and time on the basis of continuity and incompressibility. It is important to note that defining the mantle cavity geometry in this way has no effect on the external fluid flow. The mantle cavity control volume problem is entirely separate from the external flow problem, which is treated elsewhere (E. J. Anderson, W. R. Quinn and M. E. DeMont, manuscript submitted for publication).

Jet thrust was also calculated in a quasi-steady sense using the steady form of equation 11, that is:

$$T = \rho V_\mathrm{j}^2 A_\mathrm{j}\,, \qquad (12)$$

where T is steady jet thrust. This is the equation normally used to calculate jet thrust for swimming squid. When time-varying quantities, such as jet velocities and jet areas, are inserted into a steady flow equation such as this, the result is termed quasi-steady. The quasi-steady jet thrust is therefore the approximate instantaneous jet thrust if unsteady effects are negligible.

Intramantle pressure and jet velocity have commonly been related using the steady form of the Bernoulli equation:

$$\frac{p_\mathrm{m}}{\rho} + \frac{V_\mathrm{m}^2}{2} + \boldsymbol{g}z_\mathrm{m} = \frac{p_\mathrm{j}}{\rho} + \frac{V_\mathrm{j}^2}{2} + \boldsymbol{g}z_\mathrm{j}\,, \qquad (13)$$

where p_m is the intramantle pressure, V_m is the fluid velocity in the mantle, p_j is the pressure of the fluid into which the jet is issuing, $\boldsymbol{g}$ is the acceleration due to gravity and z is height measured from an arbitrary reference point. Squid investigators set z_m=z_j, assuming level swimming, assign p_j=0, and use the large-reservoir approximation, which assumes $V_\mathrm{j} \gg V_\mathrm{m}$, to obtain:

$$p_\mathrm{m} = \tfrac{1}{2}\rho V_\mathrm{j}^2\,. \qquad (14)$$

Traditionally, equations 12 and 14 have been combined, including a discharge coefficient, C_d, used to account for deviation from ideal mass flow. This results in an expression for jet thrust:

$$T = 2C_\mathrm{d}A_\mathrm{j}p_\mathrm{m}\,. \qquad (15)$$

As mentioned above, the accurate measurement of volume flow rate by image analysis methods eliminates the need for approximated discharge coefficients. The scheme presented in equations 12–15 has been used both to predict jet flow and thrust from intramantle pressure measurements from cannulated squid (O'Dor, 1988a,b; Webber and O'Dor, 1986; Johnson et al., 1972) and, in reverse, from thrust measurements of tethered squid (Trueman and Packard, 1968). Siekmann (1962) and Weihs (1977) present rigorous treatments of pulsating jet propulsion.

In the present investigation, intramantle pressure was calculated using the unsteady form of the Bernoulli equation without the large-reservoir approximation. The unsteady Bernoulli equation is the same as equation 13 with a term added to the right-hand side:

$$\frac{p_\mathrm{m}}{\rho} + \frac{V_\mathrm{m}^2}{2} + \boldsymbol{g}z_\mathrm{m} = \frac{p_\mathrm{j}}{\rho} + \frac{V_\mathrm{j}^2}{2} + \boldsymbol{g}z_\mathrm{j} + \int_{s_\mathrm{o}}^{s_\mathrm{j}} \frac{\mathrm{d}V(s,t)}{\mathrm{d}t}\,\mathrm{d}s\,, \qquad (16)$$

where $V(s,t)$ is the fluid velocity within the control volume and s is distance along a streamline through the mantle to the jet orifice, from s_o to s_j. Since intramantle fluid velocity varies with axial position, equations 13 and 16 reveal that intramantle pressure is a function of axial position in the mantle. This has obvious implications concerning data taken from cannulated squid. Intramantle pressures calculated using both forms of the Bernoulli equation were compared. It should be noted here that the effect of the acceleration of the control volume itself (the squid mantle cavity volume) has not previously been treated. Approximate calculations from our data suggest that the effect is less than 5 % of the peak pressures, but its precise treatment is encouraged for future work.

When dealing with the Bernoulli equation, it is important to know whether the flow being analyzed is laminar or turbulent. The Reynolds number in the funnel and mantle cavity may exceed 10^4 during jetting, well over the standard value of 2×10^3 for transition in steady pipe flow. As jet velocity and mantle contraction rate increase, the flow becomes more susceptible to transition. It is not, however, generally safe to apply steady transition Reynolds numbers to unsteady phenomena. The favorable shape of the funnel and a favorable pressure gradient may suppress transition. Nevertheless, if the flow inside the squid does become turbulent for any significant proportion of the jet period, a complete theoretical treatment of pressure in the mantle cavity may require the use of another form of the Bernoulli equation. It is known as the one-dimensional energy equation and includes a head-loss term and kinetic energy coefficients to deal with the more complicated nature of the flow (Fox and McDonald, 1992).

Results

Jet activity

In Fig. 2, jet activity is represented as pulses based on the times when the jet orifice was observed to open and close. It is important to note that these are not detailed time histories of orifice profile length. The plateau of each jet pulse, which has been arbitrarily assigned a value of 1, represents the duration for which the jet is approximately at its maximum opened position. The value 0 is assigned to represent periods for which the jet orifice was observed to be closed. The maximum open periods and closed periods are simply connected by straight lines. The periods of jet activity equal to 0 represent the refill

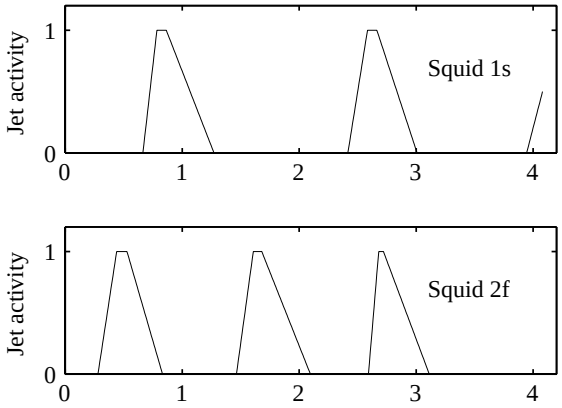

Fig. 2. Plots of jet activity comparing slow (s) and fast (f) squid, squid 1s and squid 2f. These are not detailed time histories of orifice profile length. The plateau of each jet pulse, which has arbitrarily been assigned a value of 1, represents the duration for which the jet is approximately at its maximum opened position. The value 0 has been assigned to represent periods for which the jet orifice was observed to be closed. The maximum open periods and closed periods are simply connected by straight lines. Note that, although at higher swimming speeds the jet frequency is higher, the difference in cycle period is due almost entirely to the length of the refill periods (i.e. when the orifice is closed).

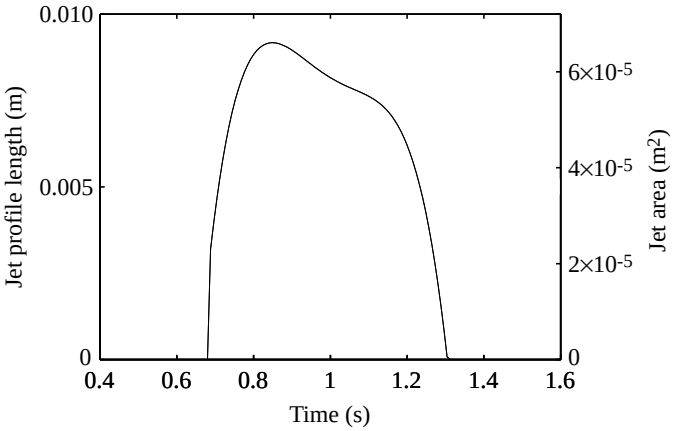

Fig. 3. Jet profile length and orifice area for the first jet period of squid 1s. The scales of the respective axes were drawn such that the curves are coincident. This linear relationship between jet orifice area and jet profile length exists because the jet orifice is modeled as a variable ellipse increasing in only one axis (equation 4).

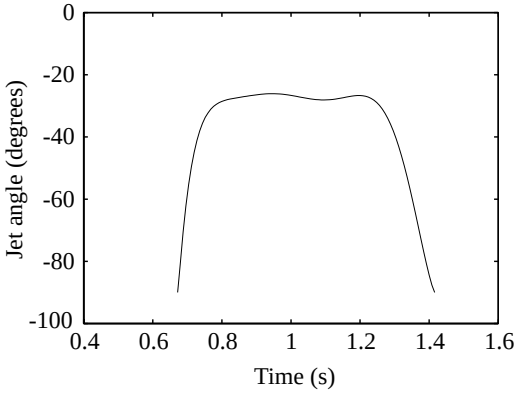

Fig. 4. Jet angle during the first jet period of squid 1s. An angle of 0° means that the jet is pointed along the squid's long axis, thereby only producing axial thrust. An angle of −90° means that the jet is pointing directly downwards, producing upward thrust.

period of the locomotory cycle. An example of more precise data for the jet orifice profile length is given in Fig. 3.

Jet cycle frequencies for the sequences shown in Fig. 2 are 0.61 Hz and 0.87 Hz. These squid (squid 1s and squid 2f) were swimming at 0.25 and 0.38 m s^{-1} respectively. Jet onset was used as the reference point by which cycle period and frequency were calculated. Closer examination of Fig. 2 reveals that the higher jet frequencies observed at higher swimming speeds are attained by shortened refill periods (jet activity=0) and only slight changes in jet period. Webber and O'Dor (1986) observed this phenomenon in *Illex illecebrosus*. For the two squid compared in Fig. 2, 92 % of the difference in locomotory cycle period is the result of the shortened refill phase in the fast-swimming squid 2f. In fact, the second jet period of the fast-swimming squid 2f is actually of longer duration (0.65 s) than either of the two jet periods in the slow swimming squid 1s (0.63 s and 0.60 s).

The jet orifice profile was visible in lateral-view sequences and had more-or-less a straight edge. Fig. 3 shows the measured length of the jet profile over the first jet period of squid 1s. The maximum observed profile length from the video sequence for this squid was approximately 9.2 mm. Direct measurements of the jet orifice profile on the same animal after death were 7.9 mm relatively unstressed and 13.0 mm stretched tightly. Fig. 3 also shows the time-varying jet area based on the elliptical intermediary areas described in the Materials and methods section (equation 4). Note that this treatment of the jet area results in a linear relationship between orifice size and jet area. Therefore, the plots of these two values, when properly scaled, are identical in shape (Fig. 3). Jet angle varied with time, but was relatively stable at approximately −30° to the long axis of the squid for the majority of the jet period (Fig. 4). Therefore, the squid appears to use its jet to produce an upward force component of 0.5 times the total jet thrust and an axial force component of 0.87 times the total jet thrust. The jet may also be applying moments to the squid. Analysis of moments requires an accurate determination of the center of mass. The overall dynamic balance in squid locomotion is examined elsewhere (Anderson, 1998).

Mantle cavity volume

Fig. 5 shows the mantle cavity volume during the swimming sequence of squid 1s and the corresponding volume flow rate. Decreases in mantle cavity volume coincide with jetting. Increases coincide with jet inactivity, during which time the squid is refilling its mantle. Mantle cavity volume changes of the order of 40 % of resting volume (68 ml) were observed in the slow-swimming squid 1s. In the fast-swimming squid 2f, mantle cavity volume changes were remarkably high, 64–94 %

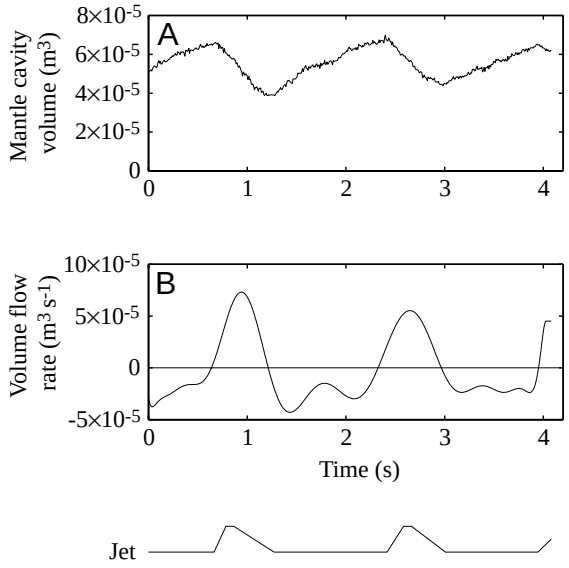

Fig. 5. Plots of mantle cavity volume (A) and volume flow rate (B) for squid 1s together with jet activity. Positive volume flow is outflow. Note that the decrease in mantle cavity volume coincides very precisely with jetting.

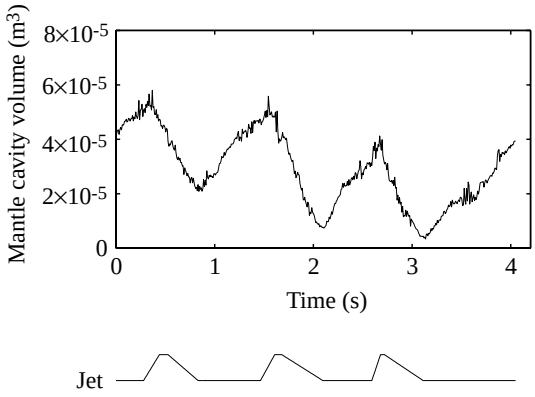

Fig. 6. Plot of mantle cavity volume for squid 2f together with jet activity. Note the consistent decrease in starting volume at the onset of sequential jet periods.

(Fig. 6). Equally remarkable was the pattern of mantle cavity volume over the entire swimming sequence of squid 2f. Following each jet, the squid failed to refill back to the volume preceding that jet (Fig. 6). During the third jet, when it expelled all but approximately 4 ml of its resting mantle cavity volume of 58 ml, the squid increased its body angle with respect to the horizontal and jetted powerfully, simultaneously wrapping its fins against itself. The squid could not continue its pattern of resting volume decrease; it needed to gain altitude and glide for a period to refill completely.

The large-reservoir approximation

The significant depletions of mantle cavity volume observed pose a challenge to the standard use of the large-reservoir approximation in the Bernoulli equation for squid. The approximation assumes that, because of the relatively large cross-sectional area of the mantle cavity compared with the jet orifice, the fluid in the mantle cavity is essentially motionless compared with jet velocity. The canonical example illustrating the large-reservoir approximation is that of a large cylindrical tank emptying through a small-diameter pipe at the bottom of the tank. A syringe with a large barrel and a small exit tube can equally illustrate the approximation and is more similar to the squid. Because of continuity and incompressibility, the relative contribution, ε, of the tank velocity term to calculated pressure compared with the contribution by the pipe velocity term, in the steady Bernoulli equation, is:

$$\varepsilon = \left(\frac{D_P}{D_T}\right)^4, \tag{17}$$

where D_P is the pipe diameter and D_T is the tank diameter. Therefore, for tank-to-pipe diameter ratios greater than 3:1, the contribution of the tank velocity to the calculated pressure is less than 1/81. In this case, neglecting the tank velocity leads to errors of less than 1–2 %. A diameter ratio of 2:1 results in a relative error in pressure of 12–13 %. These errors are acceptably small, but consider what occurs between ratios of 2:1 and 1:1. The contributions of the two terms become equal, and the large-reservoir approximation leads to large relative errors in intramantle pressure calculated from jet velocity and *vice versa*.

The model used above is slightly different from the squid. Rather than a piston-like mechanism, the squid uses mantle diameter changes to drive the fluid. This further complicates the problem since the fluid velocity at any time throughout the mantle is a function of axial position. If the squid mantle cavity is treated as a cylinder of fixed length, the velocity of fluid in the mantle would vary from zero at the end farthest from the jet to the velocity of the piston model at the end nearest the jet. Fixed length is assumed because of the relative lack of extensibility imposed upon a squid by the structure of its collagen tunic, intramuscular fibers and chitinous pen (Wainwright et al., 1982). The relative contribution, ε, of the mantle velocity term to calculated pressure compared with the contribution of the jet velocity term, in the steady Bernoulli equation, is therefore approximately:

$$\varepsilon(\xi,t) = \left(\frac{\xi}{L_m}\right)^2 \left(\frac{D_j(t)}{D_m(t)}\right)^4, \tag{18}$$

where ξ is the axial position in the mantle cavity measured from the end farthest from the jet, L_m is mantle cavity length, D_j is the jet diameter and D_m is the mantle cavity diameter. Since both mantle diameter and jet diameter vary with time, ε is a function of both position and time. The equation reveals that the large-reservoir approximation gets better as one moves away from the jet, towards ξ=0. But, for the half of the mantle closest to the jet, ξ/L_m=0.5–1.0, errors due to the large-reservoir approximation are 0.25–1 times as large as predicted in the piston-based model described above. Maximum errors in intramantle pressure occur nearest the jet.

In squid, the mantle-to-jet diameter ratio is at most approximately 3:1 near the onset of jetting and, as in the example of the fast-swimming squid 2f, can decrease to 1:1 or less at high swimming speeds. Error calculations based on actual data were made to test the large-reservoir approximation. In the slow-swimming squid 1s, maximum errors in calculated intramantle pressures neglecting intramantle flow would be 2–21 % for ξ/L_m=0.5–1.0. Errors are presented here as percentages of the average intramantle pressure calculated without the large-reservoir approximation at corresponding mantle positions over the entire jet period. This avoids misleading relative errors due to instances of calculated zero pressures that would otherwise end up in the denominator of the standard equation for relative error. Average errors in pressure over the entire jet period for ξ/L_m=0.5–1.0 would be 1–11 %. The maximum errors for the fast-swimming squid 2f would be 21–348 %, and average errors would be 5–139 % for ξ/L_m=0.5–1.0. The range of average errors is due to the uncertainty in the lengthwise distribution of mantle cavity cross-sectional area as well as the variation in pressure with mantle position.

As mentioned above, the Bernoulli equation is generally used in squid locomotion to calculate jet velocities from jet pressures. In this case, the large-reservoir approximation applied to squid 1s would lead to maximum errors of 1–8 % and average errors of 1–5 % for ξ/L_m=0.5–1.0. In squid 2f, maximum errors would be 12–155 %, and average errors would be 3–50 % for ξ/L_m=0.5–1.0. Errors in jet velocity reported here are relative to the average jet velocity calculated without the large-reservoir approximation over the entire jet period for a cannula measuring pressure at fixed positions along the region ξ/L_m=0.5–1.0.

Recall that this investigation does not include data from squid performing escape jetting. It follows that, since fast-swimming squid sometimes reduce the ratio of mantle cavity diameter to jet diameter to 1:1, the same reductions are likely to occur in escape jetting. Therefore, significant errors are expected when applying the large-reservoir approximation to link intramantle pressures and jet velocities in escape jetting.

In summary, the application of the large-reservoir approximation to squid is dubious. Its use in the analysis of squid intramantle pressure masks the physical reality that the geometry of squid can result in significant variations in pressure throughout the mantle. The approximation may be applied with reasonable accuracy for squid swimming slowly. At higher speeds, the approximation may possibly be applied in the region of the mantle cavity far from the jet. For example, jet velocity could have been calculated from intramantle pressure measured with a cannula in squid 2f with less than 10 % maximum error if the cannula had been inserted within ξ/L_m=0–0.3. This critique of the large-reservoir approximation has been presented within the realm of quasi-steady flow. Unsteady effects also affect calculated intramantle pressure, as outlined above. The results of the unsteady calculations are presented below after jet velocity calculations, which are a prerequisite to the determination of intramantle pressure.

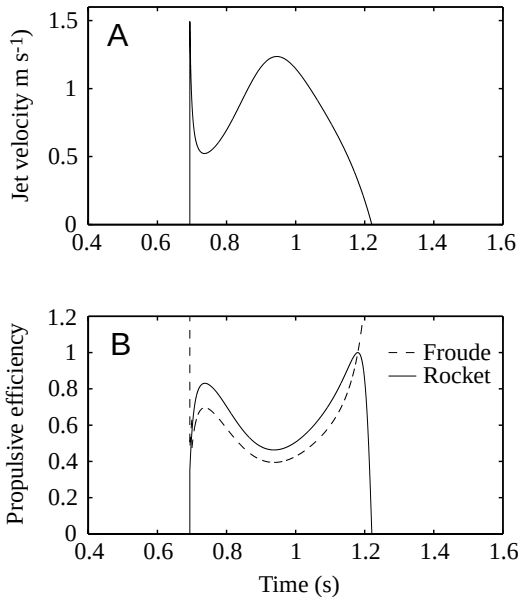

Fig. 7. Jet velocity (A) and propulsive efficiency (B) during the first jet period of squid 1s. Efficiencies calculated using the Froude (equation 6) and rocket motor (equation 7) equations are compared.

Jet velocity

Jet velocity (Fig. 7A) was calculated from the time-varying volume flow rate and jet area. The graph of jet velocity shows a large initial peak. There certainly may be an initial velocity peak when the jet opens caused by the pressure built up in the mantle; however, the height of the peak may be partially an artifact introduced by the equation used to calculate jet velocity (equation 5). The very small initial areas, which start at zero, could result in very high calculated velocities if volume flow rate, Q, is non-zero before the jet is supposed to have opened. Even a very small value for Q could have such an effect. An initially positive Q could be the result of initial backflow at the funnel/mantle valve, a slight mantle length change upon contraction, picking the wrong video frame as the starting point of jet opening or error due to the axisymmetric assumption. If the initial peak is ignored, the maximum jet velocity is approximately 1.25 m s^{-1} for the 0.2 kg squid 1s swimming at 0.25 m s^{-1}. Average jet velocity is 0.54 cm s^{-1}. Webber and O'Dor (1986) report a jet velocity of 1.4 m s^{-1} for a 0.5 kg *I. illecebrosus* swimming at 0.5 m s^{-1}.

Propulsive efficiency

Fig. 7B displays propulsive efficiency when the squid is treated as a rocket (equation 7) or as an airscrew-like propeller (equation 6). The rocket equation gives an average propulsive efficiency of 65 %. Froude efficiency averaged 56 %. Efficiencies greater than 100 %, which result in the application of the Froude efficiency equation to squid, were ignored. The fact that the efficiency calculated using the rocket efficiency equation is higher than the Froude efficiency is understandable since, as mentioned above, the rocket equation neglects fluid intake. Whole-cycle propulsive efficiency calculated from

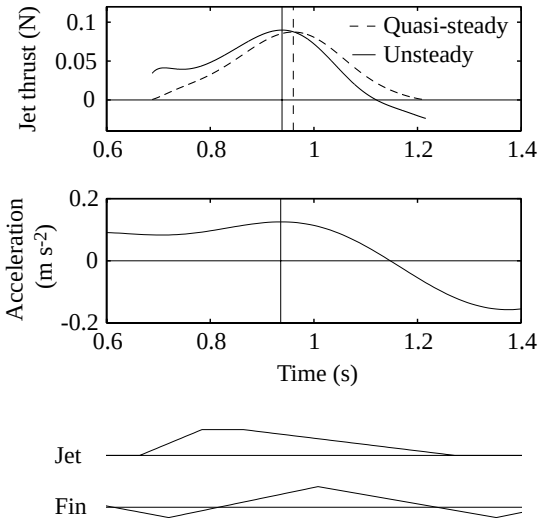

Fig. 8. Comparison of quasi-steady and unsteady theoretical jet thrust, axial acceleration, jet activity and fin activity during the first jet period of squid 1s. Peak values are marked with vertical lines. On the fin activity plot, a positive slope represents fin upstroke, and a negative slope respresents fin downstroke. Note that peak unsteady jet thrust agrees with peak axial acceleration slightly better than does peak quasi-steady jet thrust. Also, axial acceleration becomes negative before the jet period ends. The theoretical jet thrust including unsteady effects appears to be a better explanation of this event than that calculated in a quasi-steady sense. In addition, the fin is performing a thrust-producing downstroke during the period of negative acceleration. It is not, therefore, expected to contribute to the deceleration. In fact, fin thrust may explain the slight lag between the axial deceleration and the point when the unsteady jet thrust becomes negative. Drag on the squid also causes deceleration and may affect this interpretation.

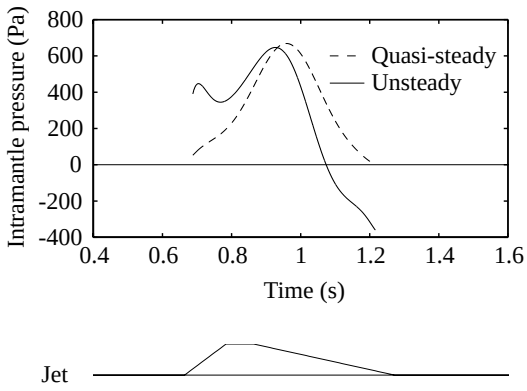

Fig. 9. Comparison of quasi-steady and unsteady theoretical intramantle pressure near the position of maximum mantle diameter during the first jet period of squid 1s.

equation 8 is 34–48 %. The range of average whole-cycle efficiency exists because refill orifice area is uncertain. Therefore, refill velocity, V_R, is uncertain. Lower refill velocities, i.e. larger refill areas, result in higher efficiency. Recall that equations 6–8 assume ideal, steady flow.

Jet thrust

Fig. 8 displays unsteady and quasi-steady jet thrust as they compare with the axial acceleration of the whole squid. Jet and fin activity are included. Average unsteady jet thrust is approximately 0.03 N, and peak thrust reaches nearly 0.09 N. Although the curves appear somewhat similar, peak thrusts for the two curves are different and occur at different times. Also, the thrust curve that includes unsteady effects becomes negative near the end of the jet period. Both the shift and the negative values of the unsteady thrust curve have a simple physical explanation, intramantle fluid accelerations. Early in the jet period, the intramantle fluid is accelerated. This leads to an early peak in the unsteady term of the momentum equation (equation 11). Near the end of the jet period, the fluid remaining in the squid decelerates, resulting in a negative force on the squid. Therefore, the unsteady term in equation 11, if plotted, would be shaped like a sine curve. Quasi-steady thrust depends only on jet velocity and volume flow rate, which are both positive for the duration of the jet and reach their maxima at approximately the same time, in the middle of the jet period. Superimposing the fluctuating unsteady term and the steady term of equation 11 yields the unsteady jet thrust curve shown in Fig. 8.

The unsteady jet thrust matches axial acceleration better than the quasi-steady thrust. First, peak thrust and peak acceleration coincide precisely (Fig. 8). This is especially significant because the peak acceleration occurs during fin upstroke, when the fins in squid 1s were not observed to contribute significantly to thrust (Anderson, 1998). It would be difficult to explain how a peak in acceleration would occur before peak jet thrust, as is predicted by the quasi-steady analysis. Second, the squid is decelerating when the quasi-steady analysis predicts positive force (Fig. 8). This deceleration begins shortly after the jet thrust from the unsteady model becomes negative. In this case, the fin is performing a thrust-producing downstroke, which could explain why acceleration does not become negative simultaneously with the negative unsteady jet thrust. Drag on the squid may contribute significantly to the observed deceleration, however, making it difficult to evaluate. Nevertheless, there is some evidence in our data for unsteady effects on jet thrust as predicted by theoretical hydrodynamics.

Intramantle pressure

The unsteady term in the Bernoulli equation has a similar effect on the calculated intramantle pressure (Fig. 9). Once again, the curve including unsteady effects is shifted to the left and becomes negative near the end of the jet period. This negative pressure is not due to expansion of the mantle. The mantle diameter is still decreasing during this time. The negative pressure is linked to the deceleration of the intramantle fluid. During the jet period, water in the mantle is moving towards the jet. Not all the water is expelled. The remaining volume is decelerated in the mantle. It was explained above that the pressure calculated without making the large-reservoir approximation and using the unsteady

Bernoulli equation is dependent on position in the mantle. Fig. 9 shows calculated intramantle pressure near the position of maximum mantle diameter. These pressures have been used, together with mantle strain rates, to produce the second genuinely *in vivo* force/velocity trajectory in animal locomotion (Anderson, 1998). The first such trajectory was accomplished by a similar analysis of scallop swimming by Cheng and DeMont (1996, 1997).

Although direct measurements of intramantle pressure are scarce and often of low temporal resolution, there are hints of the unsteady effects of Fig. 9 in published pressure measurements. Negative pressure spikes are evident in the pressure records of O'Dor (1988a), Gosline and DeMont (1985), Gosline et al. (1983) and Shadwick (1994). These measured negative pressures may simply be due to the elastic recoil of the mantle, but this does not rule out some contribution from unsteady effects. In fact, careful inspection of Shadwick's (1994) data from an escape-jetting *L. forbesi* suggests, however weakly, that pressure becomes negative an instant before the mantle diameter begins to increase. In addition to negative pressures at the end of the jet period, Fig. 9 reveals a small initial pressure spike in the unsteady case in addition to the main pressure spike. Such double spikes appear in measured intramantle pressures in some cases (Gosline et al., 1983). Shadwick (1994) also found a sharp pressure increase early in the jet period.

Discussion

Unsteady jet propulsion

Jet propulsion in squid, and undoubtedly in other organisms, is a complicated and unsteady hydrodynamic process (Daniel, 1984). This is illustrated in the present investigation by the negative thrust and intramantle pressures that occur as a result of unsteady flow relative to the control volume represented by the squid mantle cavity. It had been supposed previously that any decrease in mantle diameter is due to the contraction of circular muscles, with the exception of cases involving hyperventilation. Unsteady pressure calculations, however, suggest that negative intramantle pressures near the end of the jet period may assist/cause a prolonged 'contraction' of the mantle. Gosline and Shadwick (1983) claimed that the loading of elastic fibers in the mantle mitigates energy losses resulting from a continued contraction of the circular muscles beyond the point of maximum jet hydrodynamic performance. They argue that, during the time of least elastic loading, the circular muscles are free to put their greatest effort into producing the jet. As the diameter of the squid decreases, it would be necessary for the squid to increase its muscle contraction rate to keep volume flow rate constant because of the cylindrical geometry of the squid. Instead, volume flow rate decreases and, therefore, so does jet thrust. The elastic fibers, in contrast, continue to load regardless of the rate of contraction. Gosline and Shadwick (1983) claim, therefore, that the system opts for energy storage rather than a potentially wasteful high-power thrust event. The idea is that the circular muscles continue to contract to produce some thrust and, at the same time, potentially wasted circular muscle energy is dumped into loading elastic fibers, to be recovered during refill.

The loading theory of Gosline and Shadwick (1983) may be correct, but the unsteady picture of squid jet propulsion predicts negative pressures in the mantle during the period in which they predict that circular muscle energy is being transferred to elastic fibers. Our findings suggest that the loading of elastic fibers could be an efficient breaking mechanism of mantle deformation that capitalizes on the negative pressures in the mantle resulting from the unsteady hydrodynamics of flow in the mantle cavity. The unsteady analysis suggests that the circular muscles may actually be passive during this time.

In addition to time-base differences in intramantle pressure, the model presented here predicts variation in pressure throughout the mantle. Highly resolved, intramantle pressure measurements from many different positions along the mantle are needed for proper scrutiny and adjustment of the model.

The weaknesses of Froude efficiency

The use of Froude efficiency to determine propulsive efficiency for squid and other jet-propelled organisms is tenuous on several grounds. First, the derivations of both jet period (equation 7) and whole-cycle propulsive efficiency (equation 8) in squid did not result in the equation of Froude efficiency, even though the same assumptions used in the derivation of Froude efficiency – ideal, steady flow – were used in their derivation. Second, efficiencies calculated using the Froude equation simply do not match those calculated using equations derived specifically for squid propulsion. Froude efficiency was found to be lower than the efficiency calculated for the jet period and higher than whole-cycle efficiency. Recall that, for the 0.169 kg *L. pealei* swimming at $0.25\,m\,s^{-1}$ (squid 1s), Froude efficiency averaged 56 %, rocket efficiency averaged 65 % and whole-cycle propulsive efficiency was predicted to fall between 34 and 48 %. The 0.5 kg *I. illecebrosus* reported by Webber and O'Dor (1986) to be swimming at $0.5\,m\,s^{-1}$ with a jet velocity of $1.4\,m\,s^{-1}$ has a Froude efficiency of 53 %. The propulsive efficiency of the same *I. illecebrosus* during jetting, if treated as a rocket, is 63 %. The same discrepancy has been reported in scallop swimming. Cheng and DeMont (1996) briefly mention the weakness of Froude efficiency for predicting efficiencies in scallops and calculate efficiency using other methods. Interestingly, just as using rocket motor efficiency gives higher average efficiencies than those calculated by Froude efficiency, Cheng and DeMont (1996) found higher efficiencies in the scallop employing alternative methods.

O'Dor and Webber (1991) report total locomotory efficiency for a 0.6 kg *L. pealei* to fall between 5.9 and 34 % on the basis of swim-tunnel respirometry. Note that this is not whole-cycle propulsive efficiency; instead, it is the total efficiency of locomotion based on oxygen consumption. Propulsive efficiency would, however, set the upper bound of

total efficiency. While the comparison may be weak because of the difference in squid size, it is encouraging that the total efficiencies reported by O'Dor and Webber (1991) for *L. pealei* do not exceed the range of our calculated whole-cycle propulsive efficiencies (34–48 %).

Third, the mechanical system from which Froude efficiency is derived is significantly different from the squid jet propulsion system with regard to fluid intake and jet production. The airscrew propulsion system, from which Froude efficiency is derived, involves the continuous addition of momentum to the fluid moving through a propeller. The working fluid is never brought to rest with respect to the propeller. This results in a very efficient intake system. In fact, there are no terms representing intake losses in the Froude efficiency equation. In the periodic jetting of squid, the working fluid is brought to rest with respect to the body before each jet period begins. This is a costly process similar to an inelastic collision.

One advantage to this process, however, is that the squid can produce thrust even if its jet velocity with respect to itself is less than its velocity with respect to the surrounding fluid. Once the squid has brought the working fluid up to its velocity, any expulsion of mass from the jet will result in thrust. This is not the case for the airscrew. The jet produced behind the airscrew must have a velocity with respect to the propeller that is higher than the velocity of the flow past the propeller. This means that a squid produces less wake kinetic energy per thrust than a Froude treatment suggests, i.e. higher efficiency. For example, if a squid is moving with respect to the surrounding fluid at $0.25\,m\,s^{-1}$ and its jet velocity with respect to itself is $0.25\,m\,s^{-1}$ opposite to the direction of swimming, the jetted fluid exiting into the surrounding fluid is stationary with respect to that fluid, assuming ideal flow. There is no kinetic energy left in its wake from the jet to be dissipated into the surrounding fluid. Nevertheless, the change in momentum of the working fluid, as its velocity is increased from 0 to $0.25\,m\,s^{-1}$ with respect to the squid, produces thrust. In the case of an airscrew, 100 % efficiency is also approached when the jet velocity is equal and opposite to the velocity of the propeller through the fluid but, in contrast, no thrust is produced and propulsive efficiency is meaningless.

Finally, when the Froude efficiency equation is applied to a swimming squid, it results in periodic efficiencies of greater than 100 %. The squid-specific equations do not. This is directly related to the ability of squid to produce thrust even when jet velocity is lower than swimming velocity. Fig. 7B compares Froude efficiency with the propulsive efficiency calculated when treating the squid as a rocket during the jet period. Froude efficiency gives lower values over most of the jet period, but gives greater than 100 % efficiencies over periods near the beginning and end of the jet period, as jet velocity drops to zero. This is inconsistent with a physical understanding of how kinetic energy left in the wake affects efficiency. To illustrate this, imagine a squid swimming at $0.25\,m\,s^{-1}$ through still water with a jet velocity with respect to itself of $0.20\,m\,s^{-1}$ opposite to its swimming direction. Thrust is produced as a result of the change in momentum of the working fluid. However, when the jetted fluid exits, it is moving at $0.05\,m\,s^{-1}$ through the surrounding fluid in the swimming direction of the squid. The kinetic energy bound up in this fluid is dissipated into the surrounding fluid. Therefore, as jet velocity decreases below body velocity through the fluid, energy is wasted and efficiency drops. Astonishingly, Froude efficiency predicts greater than 100 % efficiency for this situation.

The discrepancy becomes clear upon consideration of an airscrew-like propeller. Froude efficiency is derived assuming that the propeller is acting in such a way as to propel the body. Therefore, in the case of determining propulsive efficiency for an airscrew, the fluid velocity downstream of the propeller is never less than that of the oncoming flow. Note that the derivation of Froude efficiency ignores drag due to the propeller blades. The airscrew rotation would have to be reversed to mimic the example above, but then the assumptions of Froude efficiency would no longer hold. Since an airscrew cannot produce forward thrust when jet velocity is less than its velocity through the fluid, Froude efficiency applied to an airscrew is never pushed into the greater than 100 % range to which the equation is prone when applied to squid. A sensible alteration for the Froude equation would be to place absolute value bars around the term $\Delta V/2$ (equation 6). This would result in a discontinuity in the equation, but would at least avoid efficiencies greater than 100 %. Average Froude efficiency calculated this way for squid 1s is 57 %, and simply reinforces the underestimation of propulsive efficiency during the jet period by the Froude efficiency equation (56 %, equation 6). Note that the Froude efficiency calculated from equation 6 is lower than the altered equation only because the former was calculated ignoring efficiencies greater than 100 %. The altered equation actually results in lower average efficiencies in comparison with equation 6.

The usefulness of any equation, apart from predicting accurate values, is its ability to reveal information concerning the mechanism it describes. Froude efficiency fails in both categories for squid locomotion. Most significantly, Froude efficiency fails to describe the important role that that the refill mechanism plays in lowering efficiencies in squid locomotion. Instead, it somewhat unfairly targets jet propulsion. For many years, low efficiencies in squid have been blamed on a propulsion system that relies on the acceleration of a small mass of fluid to high velocities, largely from the perspective of Froude efficiency (Lighthill, 1969). Granted, this effect in squid does contribute somewhat to lower efficiencies than would be achieved by accelerating a larger mass of fluid to lesser velocities, but the present work reveals that relatively high efficiencies can be obtained during the jet period of squid propulsion. Webb (1971) reports that propulsive efficiency in fish may be as high as 81 %. A Froude efficiency of 56 % for squid pales in comparison, but a 65 % average efficiency during jetting is only 16 % less than the reported maximum for fish. Jet propulsion, in and of itself, suddenly does not look so dramatically inefficient as has been commonly believed. It is extremely interesting that the equation for whole-cycle propulsive efficiency derived in this investigation predicts an

upper bound of 58 % on propulsive efficiency and an optimum jet velocity of 1.7 times swimming speed. Squid 1s, which was swimming at a speed that may fall in the range of migratory speeds, had an average jet velocity of 2.2 times its swimming speed. This means that squid 1s was jetting in such a way as to approach a whole-cycle propulsive efficiency as high as 56 %, just 2 % from its theoretical maximum. The fish, at 81 %, is operating at 19 % lower than its theoretical maximum. Unfortunately for the squid, however, its refill period is very costly, but perhaps the squid is making better use of the mechanisms it has available.

In conclusion, several aspects of squid jet propulsion apparently need to be reconsidered. Unsteady effects appear to be significant, and their impact on functional morphology should be further explored. Traditional approximations and assumptions in the analysis of squid locomotion, such as the large-reservoir approximation in the Bernoulli equation, may not give an accurate picture of their locomotory mechanism and fail to guide experimental technique appropriately. The variation in pressure with mantle position is a good example. Furthermore, there appears to be little basis for calculating propulsive efficiency in squid and certain other jet-propelled organisms using Froude efficiency. Treatment of the squid as a rocket motor during jetting results in a better description of the actual balance of energy. Ultimately, custom-derived equations for whole-cycle efficiency have the most to offer in the determination of the propulsive efficiency of periodic jet locomotion. The role of the unsteady jet in biology may be more sophisticated than previously believed and poses an exciting challenge for future investigation.

List of symbols

$A_j(t)$	cross-sectional area of the jet orifice
a	major axis (horizontal) of the elliptical jet orifice
$b(t)$	minor axis (vertical) of the elliptical jet orifice
C_d	discharge coefficient
CS	control surface area; the surface defined by the inner walls and the jet orifice, which surround the working fluid within the squid
$C\forall$	control volume; the space occupied by the working fluid within the squid
$D_j(t)$	jet diameter treating jet as circular
$D_m(t)$	mantle inner diameter treating the mantle cavity as a cylinder
D_P	pipe diameter in the large-reservoir example
D_T	tank diameter in the large-reservoir example
$D(\xi,t)$	outer diameter of the mantle at position ξ
dA	incremental area of the control surface, CS
$d\forall$	incremental volume of the control volume, $C\forall$
E_R	total energy required to refill the mantle cavity
E_w	total wake kinetic energy due to the jet
F	hydrodynamic force on squid due to jetting, jet thrust
$\boldsymbol{g}$	acceleration due to gravity
L_m	mantle length
p_j	fluid pressure into which the jet is issuing
p_m	fluid pressure at some position, m, in the mantle cavity
$Q(t)$	volume flow rate; out of the mantle cavity is positive
s	position along a particular streamline
s_j	position at the jet orifice along a particular streamline, s
s_o	position at the leading end of the mantle cavity along a particular streamline, s
t	time
T	thrust
$V_j(t)$	jet velocity relative to the squid jet orifice
V_m	flow velocity at some position, m, in the mantle cavity
$V_R(t)$	refill intake velocity relative to the squid intake orifice
$V(s,t)$	velocity of the working fluid within the squid along a particular streamline, s
$V(t)$	swimming speed relative to the surrounding fluid
$V(x,t)$	velocity of the working fluid within the squid along the longitudinal axis
$\forall_C(t)$	volume of the mantle cavity working fluid
$\forall_m(t)$	total fluid and tissue volume of the mantle
$\forall_{max}$	maximum volume of the total fluid and tissue volume of the mantle during a particular swimming sequence
$\forall_R$	resting volume of the mantle cavity working fluid
W	work done against drag over one locomotory cycle
z_j	height of the jet orifice
z_m	height of the mantle
ΔV	jet velocity relative to the surrounding fluid, i.e. $V_j - V$
ε	relative contribution to pressure of the velocity terms of the Bernoulli equation
η	whole-cycle hydrodynamic/propulsive efficiency
η_f	Froude efficiency
η_j	jet efficiency
ξ	axial position measured from the leading end of the mantle
ρ	fluid density

This project was funded by an NSERC (Canada) grant to M.E.D., who also received support from the Ester A. and Joseph Klingenstein fund from the Marine Biological Laboratories (MBL, Woods Hole, MA, USA) and a W. J. Fulbright Scholarship to E.J.A. We thank R. K. O'Dor at Dalhousie University, W. Quinn, J. P. Quinn, E. C. Oguejiofor and P. MacGillivray at St Francis Xavier University, T. L. Daniel at the University of Washington, S. Gallagher, M. Grossenbaugh, W. McGillis and the staff at the Rhinehart Coastal Research Center of the Woods Hole Oceanographic Institution and R. Hanlon at MBL for technical assistance and advice.

References

Anderson, E. J. (1998). The mechanics of squid locomotion. MSc thesis, St Francis Xavier University, Nova Scotia, Canada.

Batchelor, G. K. (1987). *An Introduction to Fluid Mechanics*. Cambridge: Cambridge University Press.

Cheng, J.-Y. and DeMont, M. E. (1996). Jet-propelled swimming in scallops: swimming mechanics and ontogenic scaling. *Can. J. Zool.* **74**, 1734–1748.

Cheng, J.-Y. and DeMont, M. E. (1997). A predicted *in vivo* muscle force–velocity trajectory. *Can. J. Zool*. **75**, 371–375.

Daniel, T. L. (1984). Unsteady aspects of aquatic locomotion. *Am. Zool*. **24**, 121–134.

Fox, R. W. and McDonald, A. T. (1992). *Introduction to Fluid Mechanics*, fourth edition. New York: John Wiley and Sons.

Gosline, J. M. and DeMont, M. E. (1985). Jet-propelled swimming in squid. *Scient. Am.* **252**, 96–103.

Gosline, J. M. and Shadwick, R. E. (1983). The role of elastic energy storage mechanisms in swimming: an analysis of mantle elasticity in escape jetting in the squid, *Loligo opalescens*. *Can. J. Zool.* **61**, 1421–1431.

Gosline, J. M., Steeves, J. D., Harman, A. D. and DeMont, M. E. (1983). Patterns of circular and radial mantle muscle activity in respiration and jetting of the squid. *J. Exp. Biol*. **104**, 97–109.

Houghton, E. L. and Carpenter, P. W. (1993). *Aerodynamics for Engineering Students*. New York: Halsted Press.

Johnson, W. and Soden, P. D. (1966). The discharge characteristics of confined rubber cylinders. *Int. J. Mech. Sci.* **8**, 213–225.

Johnson, W., Soden, P. D. and Trueman, E. R. (1972). A study in jet propulsion: an analysis of the motion of the squid, *Loligo vulgaris*. *J. Exp. Biol.* **56**, 155–165.

Lighthill, M. J. (1969). Hydromechanics of aquatic animal propulsion – A survey. *Annu. Rev. Fluid Mech.* **1**, 413–446.

MacGillivray, P. S., Anderson, E. J., Wright, G. M. and DeMont, M. E. (1999). Structure and mechanics of the squid mantle. *J. Exp. Biol*. **202**, 683–695.

O'Dor, R. K. (1988a). Limitations on locomotor performance in squid. *J. Appl. Physiol.* **64**, 128–134.

O'Dor, R. K. (1988b). The forces acting on swimming squid. *J. Exp. Biol*. **137**, 421–442.

O'Dor, R. K. and Webber, D. M. (1991). Invertebrate athletes: tradeoffs between transport efficiency and power density in cephalopod evolution. *J. Exp. Biol.* **160**, 93–112.

Prandtl, L. (1952). *Essentials of Fluid Dynamics*. London: Blackie & Son, Ltd.

Shadwick, R. E. (1994). Mechanical organization of the mantle and circulatory system of cephalopods. *Mar. Fresh. Behav. Physiol.* **25**, 69–85.

Shevtsov, G. A. (1973). Results of tagging of the Pacific squid *Todarodes pacificus* Steenstrup in the Kuril Hokkaido region. *Can. Fish. Mar. Serv. Transl. Ser*. 3300 (1974). From *Izv. Tikhookean. Nauchno-Issled Inst. Rybn. Khoz. Okeanogr*. **87**, 120–126.

Siekmann, J. (1962). On a pulsating jet from the end of a tube, with application to the propulsion of certain aquatic animals. *J. Fluid Mech.* **151**, 399–418.

Streeter, V. L. and Wylie, E. B. (1985). *Fluid Mechanics*, eighth edition. New York: McGraw-Hill.

Trueman, E. R. and Packard, A. (1968). Motor performances of some cephalopods. *J. Exp. Biol.* **49**, 495–507.

Vogel, S. (1987). Flow-assisted mantle cavity refilling in jetting squid. *Biol. Bull.* **172**, 61–68.

Vogel, S. (1994). *Life in Moving Fluids*. Princeton: Princeton University Press.

Wainwright, S. A., Biggs, W. D., Curry, J. D. and Gosline, J. M. (1982). *Mechanical Design in Organisms*. Princeton: Princeton University Press.

Webb, P. W. (1971). The swimming energetics of trout. I. Thrust and power output at cruising speeds. *J. Exp. Biol.* **55**, 489–520.

Webber, D. M. and O'Dor, R. K. (1986). Monitoring the metabolic rate and activity of free-swimming squid with telemetered jet pressure. *J. Exp. Biol.* **126**, 205–224.

Weihs, D. (1977). Periodic jet propulsion of aquatic creatures. *Fortschr. Zool.* **24**, 171–175.